Supplementary Information for:

Supramolecular Nanostructures Formed by Anticancer Drug Assembly

Andrew G. Cheetham[1,2], Pengcheng Zhang[1], Yi-an Lin[1,2], Lye Lin Lock[1], Honggang Cui[1,2*]

Contents

[1]Dept. Chemical & Biomolecular Engineering, Johns Hopkins University, Baltimore, MD 21218, USA.
[2]Institute for Bionanotechnology (INBT), Johns Hopkins University, Baltimore, MD 21218, USA.
[*]Correspondence to hcui6@jhu.edu

S1 Molecularcharacterization of the drug amphiphiles

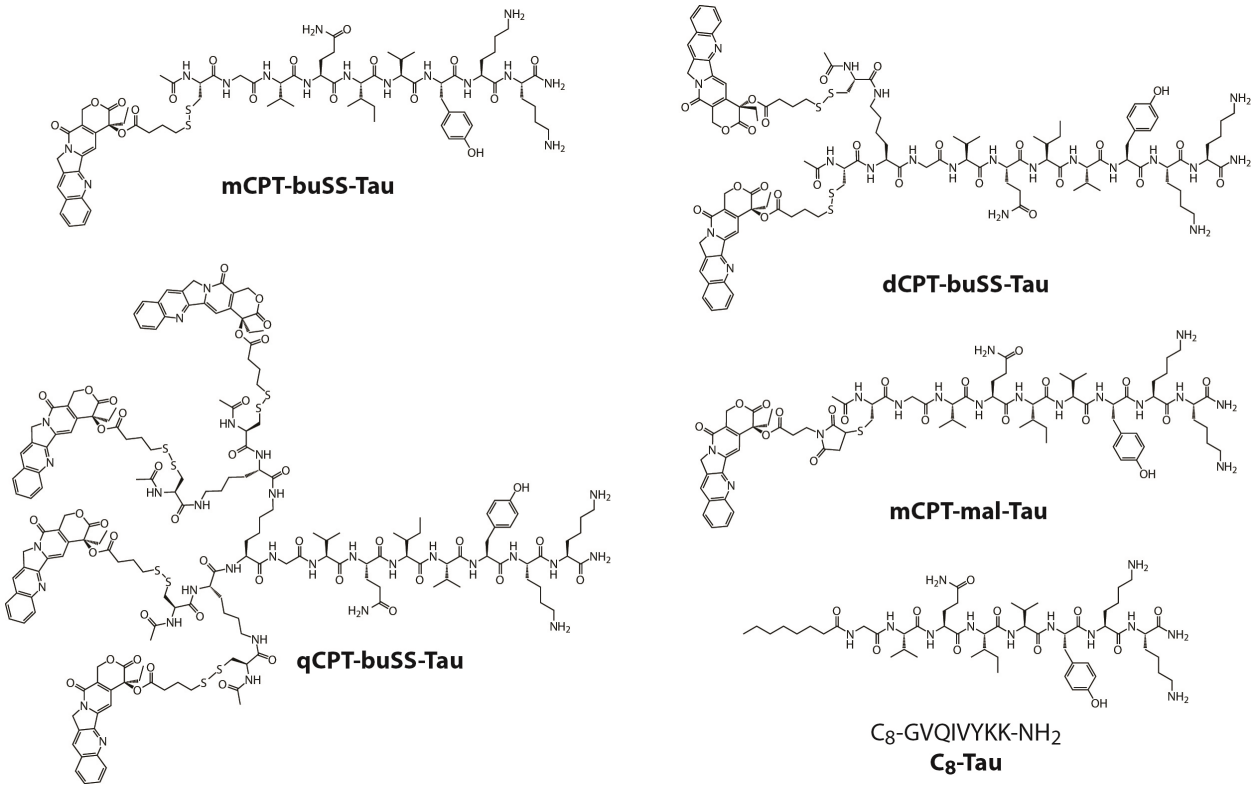

Figure S1. Molecular structures of the drug amphiphiles mCPT-buSS-Tau, dCPT-buSS-Tau and qCPT-buSS-Tau and the control molecules mCPT-mal-Tau and C8-Tau.

S1.1 mCPT-buSS-Tau

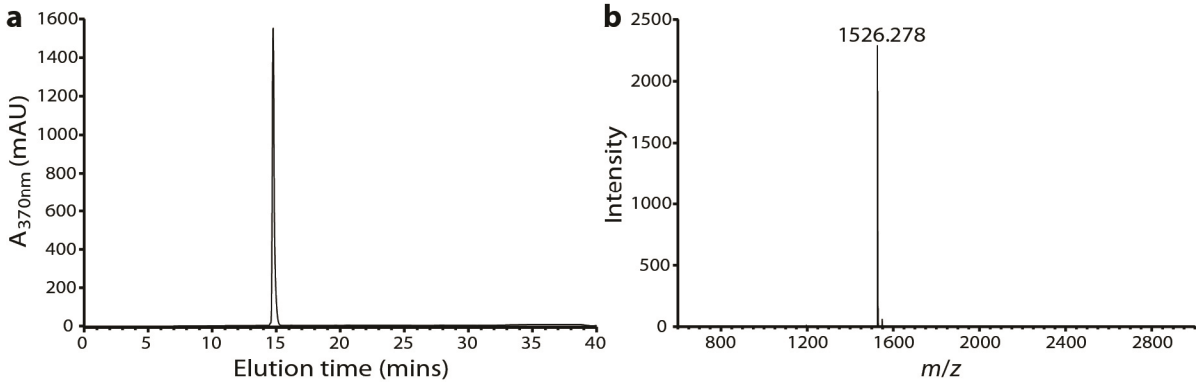

Figure S2.RP-HPLC (**a**) and MALDI-Tof MS (**b**) characterization of **mCPT-buSS-Tau**.

S1.2 dCPT-buSS-Tau

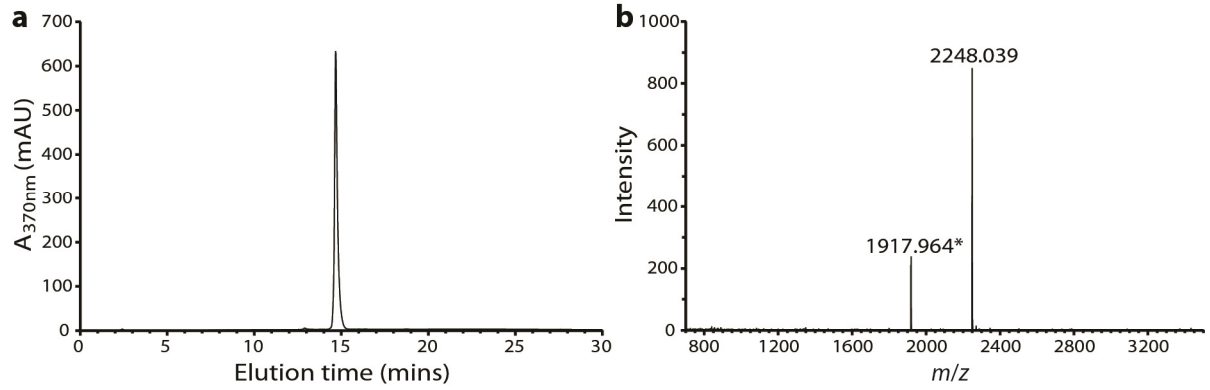

Figure S3.RP-HPLC (**a**) and MALDI-Tof MS (**b**) characterization of **dCPT-buSS-Tau**. In-source fragmentation was observed corresponding to the loss of one CPT moiety (indicated by *).

S1.3 qCPT-buSS-Tau

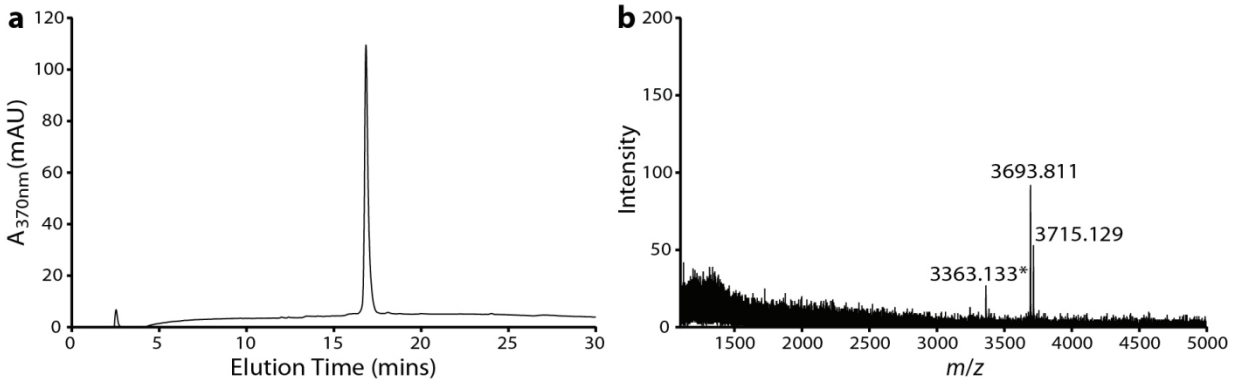

Figure S4.RP-HPLC (**a**) and MALDI-Tof MS (**b**) characterization of **qCPT-buSS-Tau**.In-source fragmentation was observed corresponding to the loss of one CPT moiety (indicated by *). Higher laser power resulted in the loss of further CPT fragments.

S1.4 mCPT-mal-Tau

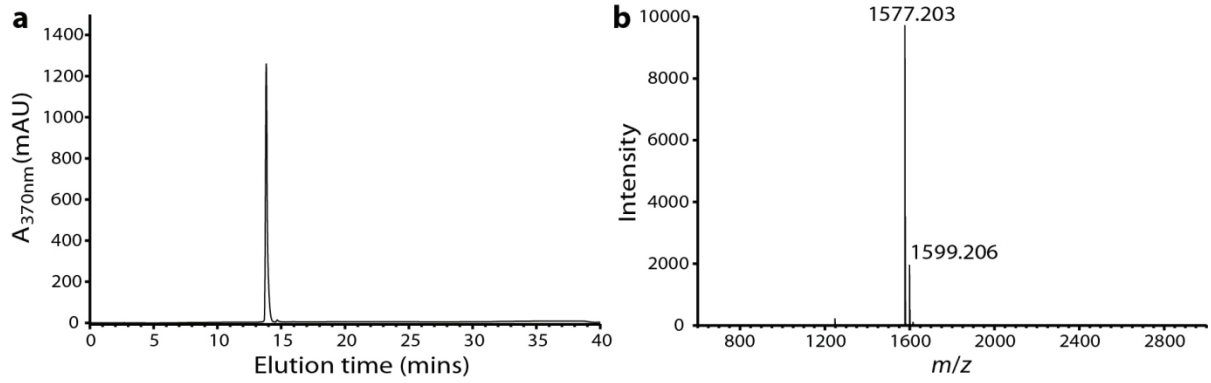

Figure S5.RP-HPLC (**a**) and MALDI-Tof MS (**b**) characterization of **mCPT-mal-Tau**.

S1.5 C_8-Tau

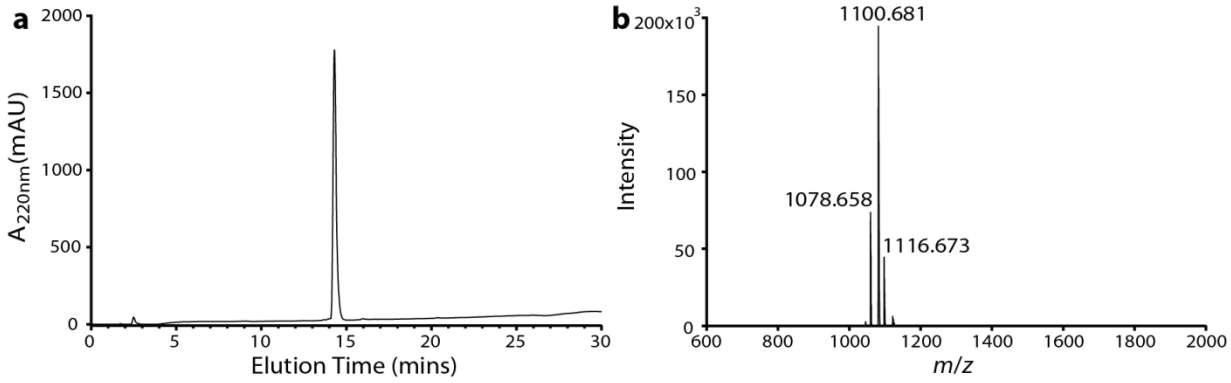

Figure S6.RP-HPLC (**a**) and MALDI-Tof MS (**b**) characterization of **C_8-Tau**.

S1.6 Drug Loading Calculations

The drug loading of the drug amphiphiles is given as the CPT weight as a percentage of the total molecular weight:

$$Drug\ loading\ (\%) = \frac{n\ \times 347.1}{M_{DA}} \times 100$$

where*n* is the number of CPT molecules conjugated and M_{DA} is the exact mass of the drug amphiphile

$$\boldsymbol{mCPT\text{–}buSS\text{–}Tau}\ drug\ loading\ (\%) = \frac{1\ \times 347.1}{1525.7} \times 100 = 23\%$$

$$\boldsymbol{dCPT\text{–}buSS\text{–}Tau}\ drug\ loading\ (\%) = \frac{2\ \times 347.1}{2246.9} \times 100 = 31\%$$

$$\boldsymbol{qCPT\text{–}buSS\text{–}Tau}\ drug\ loading\ (\%) = \frac{4\ \times 347.1}{3689.4} \times 100 = 38\%$$

S2 Characterization of the self-assembly properties

S2.1 Transmission Electron Microscopy and Cryo-Transmission Electron Microscopy

S2.1.1 Transmission Electron Microscopy (TEM) protocol

All 50 μM sample solutions were prepared from a stock solution of 1 mM conjugate in water, with the exception of **qCPT-buSS-Tau**which was prepared from a 100 μM stock solution due to its lower solubility. Samples were aged overnight prior to sample preparation. Samples were prepared by depositing 7 μL of the appropriate solution onto a carbon-coated copper grid (Electron Microscopy Services, Hatfield, PA), wicking away the excess solution with a small piece of filter paper. Next, 7 μL of a 2 wt % aqueous uranyl acetate solution was deposited and the excess solution was carefully removed as above to leave a very thin layer. Thesample grid was then allowed to dry at room temperature prior to imaging. Bright-field TEM imaging was performed on a FEI Tecnai 12 TWIN Transmission Electron Microscope operated at an acceleration voltage of 100 kV. All TEM images were recorded by a SIS Megaview III wide-angle CCD camera or 16 bit 2K × 2K FEI Eagle bottom mount camera.

S2.1.2 Cryogenic Transmission Electron Microscopy (Cryo-TEM) protocol

Cryogenic TEM imaging provides a means of visualizing structures as they exist in solution, rather than how they present upon drying and staining in conventional TEM imaging. Accordingly, this technique can be used to verify that the structures observed through conventional TEM are real and not artifacts of the preparation process. While cryo-TEM can be performed at concentrations similar to those for conventional TEM, higher concentrations allow more rapid visualization of the structures and reduce the likelihood of damage to the vitreous ice film caused by the electron beam during imaging. This potential for damage is also a limitation in the highest resolution that can be obtained, since a higher magnification would result in the electron beam being concentrated on a much smaller area. Due to this higher intensity, degradation of the vitreous ice film occurs much more rapidly making image capture extremely difficult or impossible. Accordingly, high magnification images were recorded using conventional TEM imaging techniques.

Cryogenic TEM imaging was performed on the FEI Tecnai 12 TWIN Transmission Electron Microscope, operating at 80 kV.**mCPT-buSS-Tau** and **diCPT-buSS-Tau** were imaged at 1 mM, whereas **qCPT-buSS-Tau** was imaged at 100 μM. 3-5 μL of sample solution was placed on a holey carbon film supported on a TEM copper grid (Electron Microscopy Services, Hatfield, PA). All the TEM grids used for cryo-TEM imaging were treated with plasma air to render the lacey carbon film hydrophilic. A thin film of the sample solution was produced using the Vitrobot with a controlled humidity chamber (FEI). After loading of the sample solution, the lacey carbon grid was blotted using preset parameters and plunged instantly into a liquid ethane reservoir precooled by liquid nitrogen. The vitrified samples were then transferred to a cryo-holder and cryo-transfer stage that was cooled by liquid nitrogen. To prevent sublimation of vitreous water, the cryo-holder temperature was maintained below -170°C during the imaging process. All images were recorded by a 16 bit 2K × 2K FEI Eagle bottom mount camera.

S2.1.3 Additional TEM images of qCPT-buSS-Tau

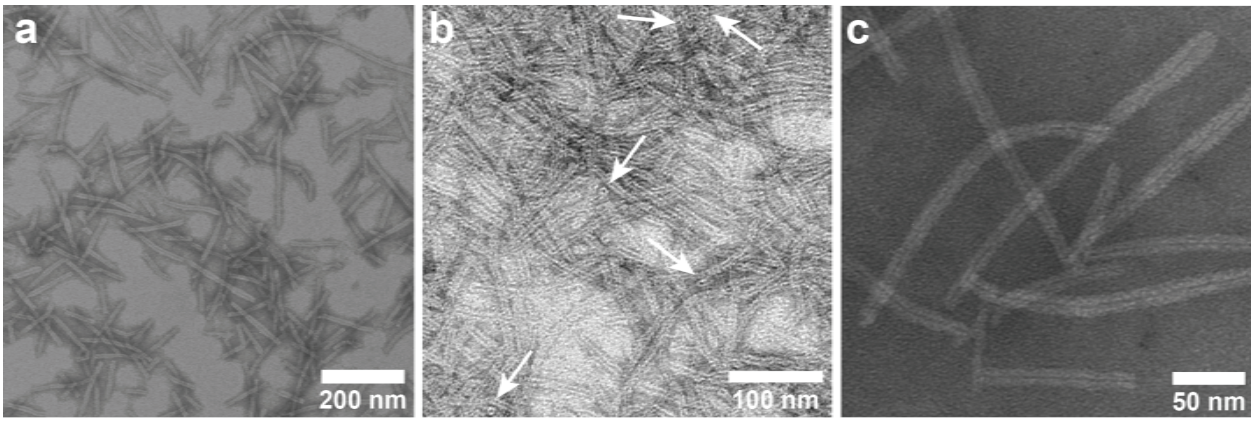

Figure S7. Additional TEM images of **qCPT-buSS-Tau** showing the adopted nanotube morphology (**a**-**c**). The tubular ends of each nanotube are indicated by white arrows (**a** and**b**). Sample concentration in each image was 50 μM. Uranyl acetate (2 wt %) was used as negative stain.

S2.1.4Self-Assembly of mCPT-mal-Tau and C_8-Tau

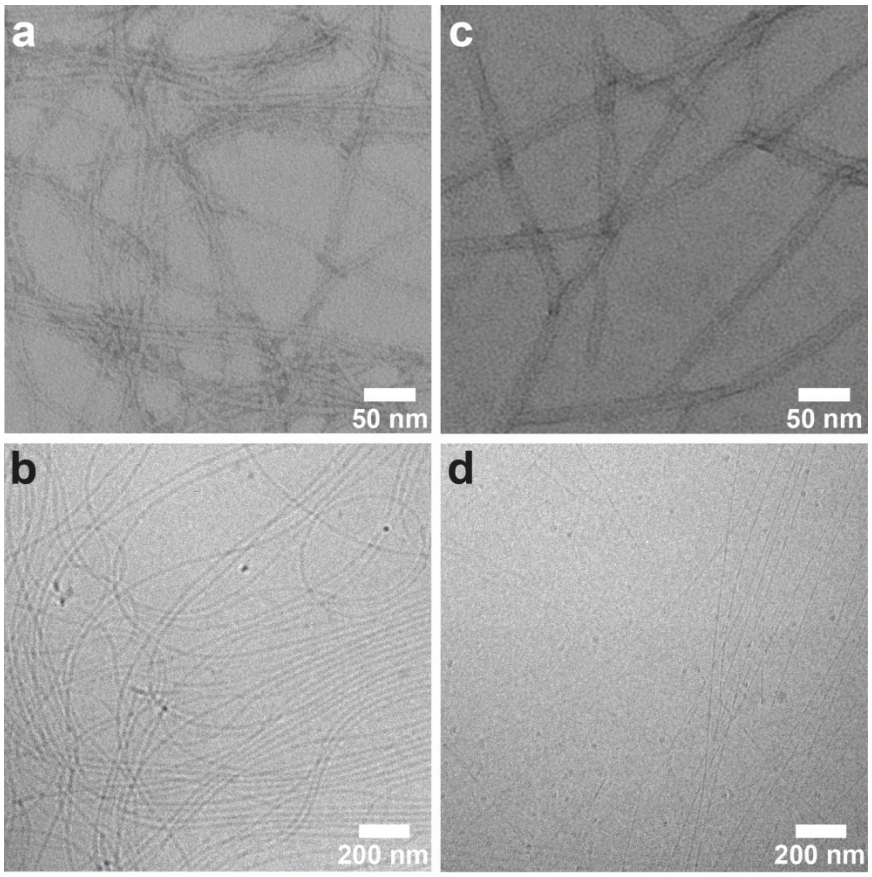

Figure S8.TEM characterization of the control amphiphiles, **mCPT-mal-Tau** and **C_8-Tau**. At 50 μM in water, mCPT-buSS-Tau can be observed to form long cylindrical nanofibers of width 5.4 ± 0.9 nm (**a**), with cryo-TEM at 1 mM showing similar structures (**b**). **C_8-Tau** was seen to form fibrous structures of varying widths at 50 μM(between 8 and 18 nm) that appear to be composed of one or more narrower fibers (**c**). Cryo-TEM at 1 mM shows fibers with widths of 9.0 ± 1.2 nm (**d**)

S2.2 Circular Dichroism (CD) Spectroscopy

CD spectra were recorded on a Jasco J-710 spectropolarimeter (JASCO, Easton, MD) using a 10mm path length Spectrasil® quartz UV-Vis absorption cell (Starna Cells Inc., Atascadero, CA). Background spectra of the solvents/buffer were acquired and subtracted from the sample spectra. Collected data was normalized with respect to sample concentration and β-sheet forming residues.

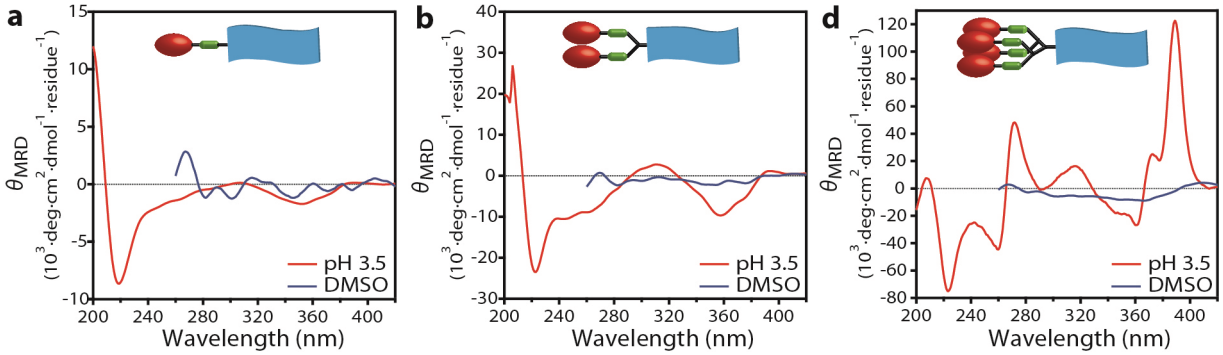

Figure S9.CD spectra **mCPT-buSS-Tau** (**a**), **dCPT-buSS-Tau** (**b**) and **qCPT-buSS-Tau** (**b**) at pH 3.5 (1 mM HCl) and in DMSO, showing persistence of the nanostructures under more acidic conditions and their existence as single molecules in DMSO.Both **mCPT-buSS-Tau** and **dCPT-buSS-Tau** show little to no signal in DMSO, whereas **qCPT-buSS-Tau** shows a relatively stronger signal. All solutions were 1 µM, with the exception of **qCPT-buSS-Tau** which was 500 nM in DMSO.

S2.3 Fluorescence Spectroscopy

Fluorescence spectra were recorded on a Fluorologspectrofluorometer (Horiba JobinYvon Inc., Edison, NJ) in a 10mm path length quartz fluorometer cuvette (Starna Cells Inc., Atascadero, CA). Samples were excited at 350 nm, monitoring the emission from 365 to 600 nm with a slit width of 2 nm.

S2.3.1Short incubation dilution study

In order to determine the short-term stability of the conjugates towards dilution, we conducted fluorescence measurements on a series of dilutions. Upon self-assembly the CPT fluorophores will experience static quenching of their fluorescence,[1] providing a means to determine the point at which dissociation of the structures occurs. Longer incubation times on the order of several hours were not possible as hydrolytic degradation was found to occur, complicating the data analysis.

Samples in 10 mM sodium phosphate buffer were prepared from 1 mM stock solutions in water (100 µM for **qCPT-buSS-Tau**) and allowed to equilibrate for an hour before analysis. 200 µl of sample solution was gradually diluted by removal and addition of an equal volume of buffer solution, recording the emission spectrum after 2 minutes of equilibration. The emission intensity at 430 nm was normalized with respect to concentration and plotted on a semi-log plot (Figure S10).

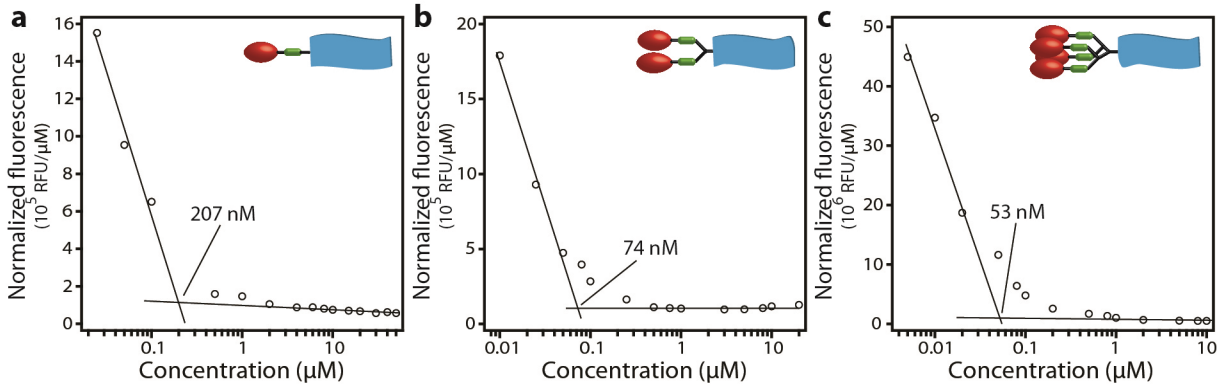

Figure S10. Fluorometric determination of the short term stability towards dilution for **mCPT-buSS-Tau** (a), **dCPT-buSS-Tau** (b) and **qCPT-buSS-Tau** (c) in 10 mM sodium phosphate.

S2.3.2Emission spectra of the drug amphiphiles

The fluorescence spectra of the drug amphiphiles (1 μM in 10 mM sodium phosphate) show an emission maximum in the 430 nm region (Figure S11), consistent with the CPT having the closed lactone form rather than the open carboxylate (which emits at 446 nm)[2].It can also be observed that the emission intensity at the maximum does not increase linearly with the number of CPT molecules each DA possesses, being less than would be expected based on simple addition. This arises due to an increase in static quenching caused by the closer proximity of the CPT molecules, withthe greatest effect being seen for **qCPT-buSS-Tau**, which also exhibits a 5 nm hypsochromic shift relative to **mCPT-buSS-Tau** and **dCPT-buSS-Tau**.

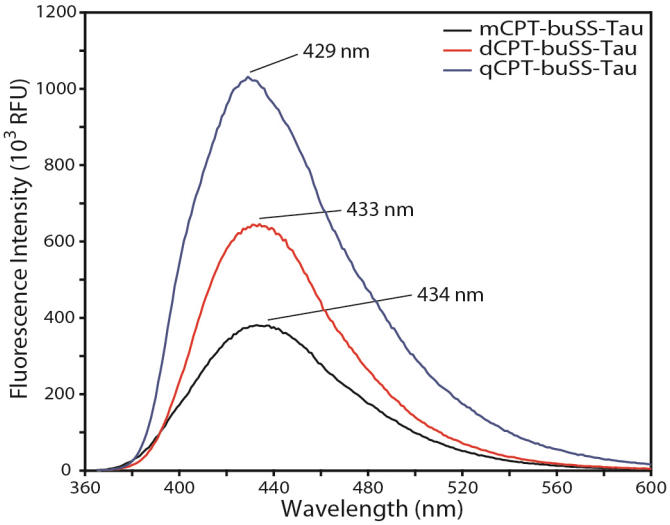

Figure S11. Fluorescence spectra of1 μM solutions of **mCPT-buSS-Tau**, **dCPT-buSS-Tau** and **qCPT-buSS-Tau** in 10 mM sodium phosphate (λ_{em} = 350 nm).

S3 Degradation study of the CPT Drug Amphiphiles

The degradation of **mCPT-buSS-Tau**, **dCPT-buSS-Tau,qCPT-buSS-Tau** and **mCPT-mal-Tau**in the presence or absence of GSH was evaluated using RP-HPLC. Briefly, 4 μM conjugate solutions in deionized water were freshly prepared before the experimentand diluted to 2 μM with sodium phosphate buffer (pH 7.4, 20 mM) with or without GSH (20 mM). The solutions were incubated at 37^{o}C and sampled at 0.5, 1, 2, 4, 6, 8, 10, 12, 24, and 48 h. The samples wereacidified by the addition of 0.2 μl of 2M HCl, flash frozen with liquid nitrogen and stored at -30^{o}C until analysis. To evaluate the effect of self-assembly on the degradation of the conjugates, the study was repeated using 20μM**mCPT-buSS-Tau**under the same conditions. The amounts of the remained conjugates were monitored by RP- HPLC using the following conditions: Varian Pursuit XRs C_{18} (5 μm, 150 × 4.6 mm); 362 nmdetection wavelength; 1 ml/min flow rate; the gradient began at 68% of mobile phase A (0.1% aqueous TFA) and 32% of mobile phase B (acetonitrile containing 0.1% TFA) at 4 minutes to 10% mobile phase A to 90% mobile phase B at 16 minutes and held for another 3 minutes. Data were plotted as a percentage of the original concentration.

S4 Cytotoxicity study of the CPT Drug Amphiphiles

The cytotoxicity of all synthesized conjugates was evaluated on a human breast cancer cell line (MCF-7), and two rat gliosarcoma cell lines (9L and F98L). Further evaluation of **dCPT-buSS-Tau** was carried out on murine ovarian cancer cell line (ID8),human cervical cancer cell line (TC-1), human lung cancer cell lines (A549 and H82), andhuman breast cancer cell line (MDA-MB-231). Briefly, cells were initially seeded into 96-well plates at 5000 cells/well and incubated in the medium – DMEM containing 10% FBS and 1% of an antibiotics solution (penicillin and streptomycin) – for 12 hoursat 37°C in a 5% CO_2 atmosphere (Oasis CO_2 incubator, Caron, Marietta, OH). The medium was then replaced with freshly prepared medium containingvarying concentrations of conjugates using free camptothecin as control, and incubated for a further 48 hours. Cell viability was determinedusing theSRB assay (Sigma-Aldrich, USA) according to the manufacturer's instructions. The exception to this protocol was for the H82 cell line, which was incubated for 72 hours and used the MTT assay (Invitrogen, USA) according to the manufacturer's instructions.The IC_{50} (the half maximal inhibitory concentration) values for each drug conjugate were obtained by fitting the data using the sigmoid or Hill equation curve analysis functions within IGOR Pro (Wavemetrics Inc., Lake Oswego, Or).

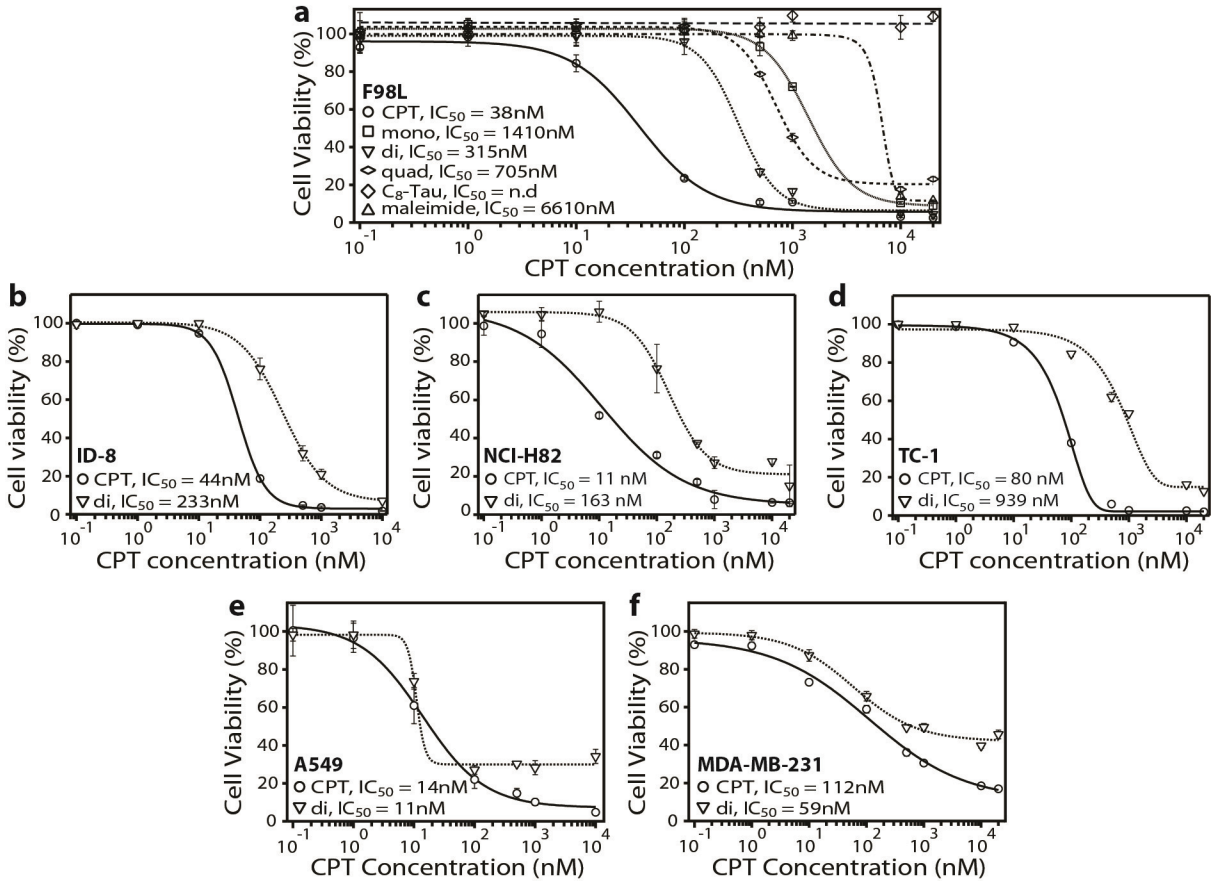

Figure S12.*In vitro* dose-response relationship study of the DA molecules against rat F98L gliosarcoma (a) cells, and **dCPT-buSS-Tau** against murine ID-8 ovarian cancer (b), human NCI-H82 small cell lung cancer (c) and human TC-1 cervical cancer (d) cellshuman A459 non-small cell lung cancer (e) and human MDA-MB-231breast cancer (f). All cancer cells were incubated with the appropriate DA molecules for 48 hours and cell viability was determined by SRB assay (n.d. = not determined).

In the wider cytotoxicity screen of **dCPT-buSS-Tau**, comparable activity to CPT was observed against murine ID8 ovarian cancer, human NCI-H82 small cell lung cancer, and A459 non-small cell lung cancer cell lines, with moderate activity against human TC-1 cervical cancer and MDA-MB-231 invasive breast cancer.

9L, F98L, A549,H82, TC-1 and ID8 cancer cell lines were kindly donated by the Hanes Lab (Johns Hopkins University); MCF-7 and MDB-MB-231 breast cancer cell lines were a generous gift from the Konstantopoulos Lab (Johns Hopkins University).

[1]M. Ogawa, N. Kosaka, P. L. Choyke, H. Kobayashi, H-type dimer formation of fluorophores: A mechanism for activatable, in vivo optical molecular imaging, *ACS Chem. Biol.***2009**, *4*, 535-546.

[2]I. Chourpa, J. M. Millot, G. D. Sockalingum, J. F. Riou, M. Manfait, Kinetics of lactone hydrolysis in antitumor drugs of camptothecin series as studied by fluorescence spectroscopy,*Biochim. Biophys Acta-Gen. Subjects,* **1998***,1379*, 353-366.